Modeling and Validation of the Human Liver and Kidney Models

S. Umale, C. Deck, N. Bourdet, M. Diana, L. Soler, R. Willinger

Abstract The objective of this study is to develop robust finite element models of the liver and kidney. The organs are modeled for the first time as hyper viscoelastic materials and with individual constituents of each (viz. the capsule and veins). To characterize the tissues, static and dynamic experiments were performed on individual parts of the porcine abdominal organs, such as capsule, vessels and parenchyma and hyper elastic, visco elastic and hyper viscoelastic materials in the form of Ogden, Mooney Rivlin and Maxwell materials were developed for each. These material models were further used to develop the finite element model of human organs. To validate these models in vitro dynamic tests on porcine kidneys were performed, whereas dynamic impact test data from the literature on human liver were used. Experiments were reproduced with the numerical approach in the LS Dyna explicit solver. The developed models are observed to reproduce the injuries of the organ to a great extent in terms of acceleration and peak force of the impactor as well as lacerations sustained by the organ during the experiments. The developed models are robust and can be integrated with the available human body finite element models to simulate accidents and to predict or simulate injuries.

Keywords liver FE model, kidney FE model, impact experiment, capsule laceration, injury reconstruction.

I. INTRODUCTION

Blunt abdominal trauma is most common in poly-traumatized patients and after neurocranial trauma it is one of the major determinants of early death in these patients. Evaluating patients who have sustained blunt abdominal trauma remains one of the most challenging and resource-intensive aspects of acute trauma care. Research by Augenstein et al. [1], Rouhana [2], Lau et al. [3] and Carnoma et al. [4] reveals that in vehicle trauma, the liver, spleen and kidneys sustain the most fatal injuries after the brain. According to Elhagediab et al. [5] the liver is the most vulnerable abdominal organ (about 38%) followed by the spleen (23%) and kidneys (4%). Scollay et al. [6] investigated 783 patients suffering from abdominal trauma over 11 years and observed that the damage was worse in patients with advanced age, multiple injuries and those requiring an immediate laparotomy; liver trauma accounted for a mortality of 22%. The liver and kidney are the most studied human body organs after the brain; however, the spleen is rarely studied due to the vexatious fact that it is always glutted with blood and even a small leak causes gushing of blood. From a biomedical aspect to develop virtual simulators and surgical tools, it is important to have accurate models of the abdominal organs which can replicate their realistic mechanical behavior. This study aims to provide a better understanding of the abdominal organs and develop models that will help to predict abdominal injuries.

Nicolle et al. [7] reported that some finite element models of the whole human body used in automotive safety research have been developed with a detailed abdomen: the WSU model from the Wayne State University [8] and its derivative TAKATA model [9-10], the Ford model from Ford Motor Company [11-13] , the H-model from ESI Group [14], the Humos model from the HUMOS European Consortium [15] and the THUMS model from Toyota Motor Corporation and Toyota Central R&D [16-17]. In all these models the liver, kidneys and spleen are modeled separately while the rest of the abdomen including stomach, pancreas, small and large intestine, gallbladder, bile ducts, ureters, rectum and adrenal glands, are usually modeled together as one or several bags under pressure [8] or an interstitial continuous solid mesh [12]. Usually a simple elastic or linear viscoelastic model is chosen to represent the mechanical behavior of these organs. Therefore, these models are not able to describe the nonlinear stress strain relationship observed by

*S. Umale, PhD, C. Deck, PhD Researcher, N. Bourdet, PhD Researcher & Prof. R. Willinger (tel: +33 (0) 3 68 85 29 23; fax: +33 (0) 68 85 36; email: remy.willinger@unistra.fr) are affiliated with IMFS, Biomechanical Systems Transport and Safety, University of Strasbourg.
M. Diana, MD and L. Soler, PhD are affiliated with IRCAD- Institut de Recherche contre les Cancers de l'Appareil Digestif, Strasbourg

soft tissues. In the WSU model [8] and TAKATA model [9], the Zener material model is made nonlinear by making the model parameters dependent on the volume change but not on the deformation. And although the liver, kidneys and spleen are well detailed geometrically in the Ford model, there is surprisingly no distinction made in their material properties. This illustrates the importance to characterize the mechanical properties of abdominal organs and to develop a validated model of each.

The literature review revealed that quite a few studies were done to characterize the abdominal organ tissues using various experimental protocols viz. tension, compression, shear, transient elastography, ultrasound, etc. Most of the studies aimed to characterize the tissue so as to aid in diagnosis of diseases. Also all the tests were done at various frequencies and strain rates so it is difficult to compare the results. Therefore, characterization experiments were performed on individual constituents of the liver and kidney. The results of the experimental tests were previously published in Umale et al. [18-19] and Chatelin et al. [20]. In the present study the results from these characterization experimental studies are used to develop the finite element models of the human liver and kidney.

II. MATERIALS and METHODS

The methodology of the study consists of characterization experiments on Glisson's capsule, hepatic vessels, liver parenchyma, renal capsule and renal cortex, and developing material models for each. The next step involves using the developed material models and the geometries to develop finite element models of the human liver and kidney with individual constituents. To validate the models dynamic experiments were performed by impacting the kidneys with a solid impactor but the human liver FE model was validated with the data of dynamic experiments obtained from the literature [22]. The same experiments were reconstructed with the FE models in the LS Dyna environment by altering material properties and using relevant material models of each of the organ components.

Experimental Testing (example)

The experiments were carried out on 9 kidneys of female pigs which were obtained from IRCAD. The organs were removed from the porcine body by performing total nephrectomy on anesthetized specimen, as per ethical standards. The organs were then wrapped in a surgical towel, soaked in saline solution, packed and transported to laboratory within 30 minutes in an ice box maintained at a temperature of 4-60C. All the tests were carried out on fresh organs without preconditioning, at room temperature (about 240C) and within 2 to 4 hours of postmortem to reduce the postmortem effect as much as possible.

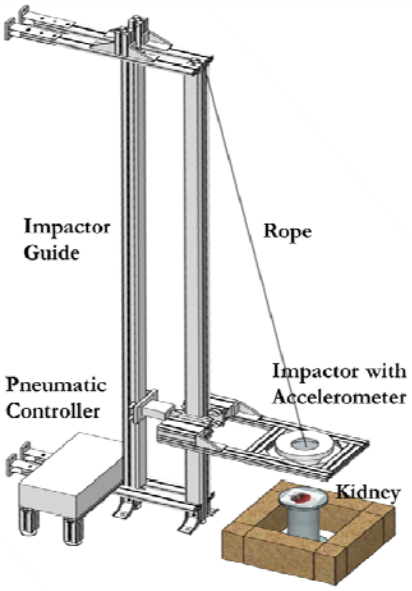

Figure 1. Schematic representation of the kidney impact test setup

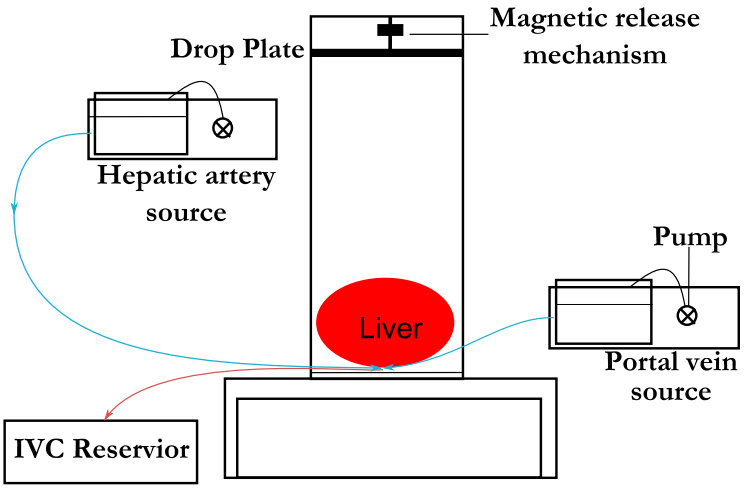

Figure 2. Schematic representation of the liver impact test setup with perfusion system.

Before performing the experiments the mass and dimensions of each of the kidneys were measured. The average mass of the 9 kidneys on which tests were performed was 48±7.25g. The dimensions and mass were incorporated into the FE model to attain the same structure as the kidneys. The kidneys were then

placed on the anvil base to be impacted by the impactor. The schematic representation of the experimental setup used for the impact tests is shown in Figure 1. The setup consists of an impactor guide which was controlled by a pneumatic mechanism. The impactor guide was lifted to desirable height to get sufficient and constant velocity (2m/s) for the impactor to impact the kidney. The impactor was placed on the guide and was tied with a rope to constrain the motion of the impactor after impact. The impactor was mounted with a KISTLER 3D accelerometer, which assisted in recording the acceleration during impact at 50 kHz. The impactor which weighed 2.5kg was released along with the guide to impact the kidney placed on the rigid anvil. The acceleration of the impactor was recorded for the impact and the peak force was calculated using the mass of the impactor. Using a high speed camera the fracture propagation of the capsule was also recorded.

In the study by Sparks et al. [21], internal pressure of the liver was used to predict the liver injury during blunt trauma. 14 human livers of healthy post mortem human specimens (PMHS) were impacted ex vivo at different velocities to determine various parameters such as peak tissue pressure, peak vascular pressure and peak impact force at the point of impact. All the organs were obtained and tested within 36 hours of death from the human cadavers with an average age of 67±16 years. The average organ mass was 1992±921 grams. The schematic diagram of the drop tower setup used to impact the human livers is shown in Figure 2. As shown an ex vivo liver perfusion system was also developed to reproduce physiological pressures in the liver vascular system and tissue. The drop tower included 23.4kg two-layered impact plates composed of steel and aluminum; accelerometers and load cells were mounted on both. The plate was released from the desired height using an electromagnetic trigger mechanism. The plate was maintained within 0.2^0 of horizontal level during the compression phase even in the highest energy tests, indicating that the irregular shape of the livers did not cause a significant amount of plate rotation or frictional loss in the bearings due to that rotation. The parameters such as peak force, peak strain, tissue pressure, etc. were reported along with the injury description of each organ.

Computational Modeling (example)

The 3D geometry of the human liver and kidney was obtained from the IRCAD online repository. The models though reconstructed from porcine kidneys can be used as the human model, as the kidneys for human and porcine are similar in shape, size, as well as material aspect [22]. The kidney segmentation geometry only consisted of the cortex as shown in Figure 3(a), whereas the medulla and pelvis were absent in the scans. It was not possible to use the geometry in the current form as it was hollow. So segmentation geometry was cleaned by deleting the inner surface elements and the enclosed volume was created by closing the open end of the kidney. The surface mesh of the kidney was then cleaned and adjusted until no failure for the criteria such as minimum and maximum element size, aspect ratio, warpage, skew, jacobian, etc. were observed. The surface mesh (shown in Figure 3(b)) was then used to create the solid tetrahedral mesh serving as the kidney cortex and the capsule of the kidney. The kidney FE model consisted of 1566 triangular shell elements and 5754 tetrahedral solid elements. The capsules, i.e. the shell elements, were modeled with a thickness of 0.05mm [19].

The kidney capsule and kidney cortex were characterized mechanically in Umale et al. [19] under static tension and static compression respectively. Using the results, the renal capsule was modeled with MAT 123 which is an elastic material with failure, whereas, the cortex was modeled with MAT 77H which is a hyper viscoelastic material with Mooney Rivlin and Maxwell model parameters. The Mooney Rivin hyper-elastic material parameters were obtained from compression results, whereas the viscoelastic parameters (Maxwell material) were obtained from the results of shear tests on liver parenchyma by Chatelin et al. [20]. The kidney model was then allowed to fall freely under the influence of gravitational force and the geometry was then extracted so as to obtain the geometry on a flat base as in the case of the experiments. The kidney FE model was scaled to match the dimensions and mass of the kidney for each experimental case. The circular flat base and a circular flat impactor were modeled with 150mm and 120mm diameter similar to that of the experiments. The density of the impactor was adjusted to weigh 2.5kg. The contacts were defined for the capsule and the cortex with the impactor and base plates as surface-to-surface contact with the static and the dynamic coefficient of friction to be 0.5 and 0.45 respectively. The impactor was supplied with an initial velocity of 2m/s and the acceleration of the impactor was recorded. The simulation setup is shown in Figure 4 and the material properties for all the materials are tabulated in Table 1. In case of kidneys the objective was to match the acceleration plots as in

experiments whereas for liver model it was to match the peak force reported in the literature. It was tried to fit the results for one of the impact experiment cases and then the same parameters were used to reconstruct the remaining cases. In the characterization experiments the tissues were tested statically; for lower strains the stiffness offered by tissues was much less. It was not possible to work with such a low stiffness. Also, there is an LS Dyna limitation that the material parameters should be positive, which also resulted in the change of material parameters, especially for kidney cortex and liver parenchyma. Therefore for the liver parenchyma and kidney cortex the characterization experimental curves were multiplied by a factor of 2 and the material parameters were fitted again; with a different set of stiffer parameters the simulations were carried out. For 20 times the original values of stress strain curve, the model parameters obtained for both liver parenchyma and kidney cortex showed stable results. Similar iterations were carried out for capsule material at the same time by increasing the elastic modulus of the capsule.

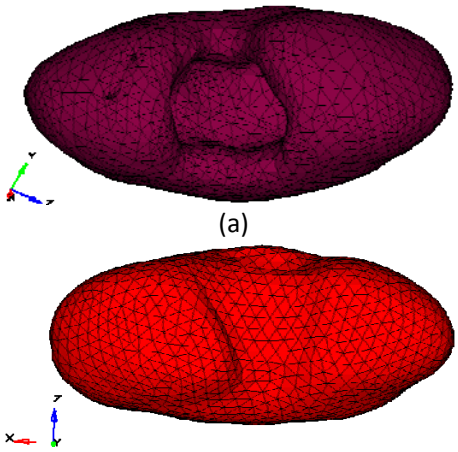

Figure 3. (a)Kidney Segmentation Geometry (b) The developed kidney FE Model.

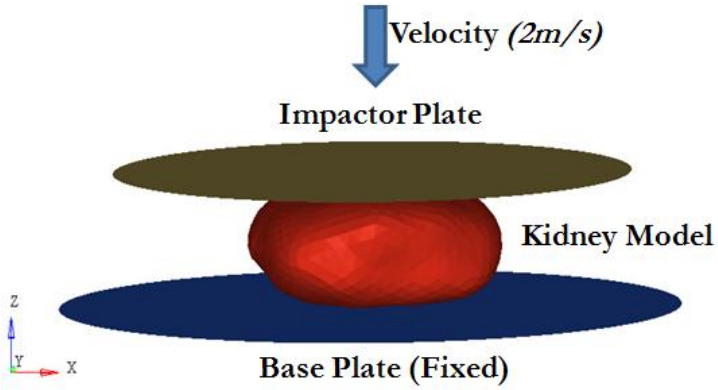

Figure 4.FEM of liver impacted with a rigid impactor in LS Dyna environment.

For the liver, the geometry from segmentation was also imported in HyperMesh software to create the liver surface mesh with triangular elements. To develop the model without vessels, the enclosed liver surface was used to create solid tetrahedral elements inside which served as the liver parenchyma. To develop the model with vessels, the portal vein geometry was obtained, which had poor geometry with very small element size. Also, some branches of the vein lacked the cross-section and only had some planar elements (Figure 5). An approximation approach was therefore adopted to recreate vein mesh geometry. The vein diameters and the lengths were mapped with the help of nodes of the vein from the segmentation data. The diameters were then dragged to follow the path of the corresponding lines of each and the cylinders were created. These cylinders were joined according to the geometry of the original veins near the joints to create an enclosed mesh of the veins as shown in Figure 6. The number of elements in the original vein geometry was 16946, whereas the vein mesh developed by dragging of circles had 3478 elements, thus providing simplicity of structure as well as reduction in calculation time with a small compromise over geometry. The meshes of liver surface and portal vein were then combined to create an enclosed volume which was modeled with solid tetrahedral elements forming the liver parenchyma as shown in Figure 7. The mesh of all constituents (capsule, parenchyma and veins) of liver was joined such that the boundary was developed with shared nodes with a continuous mesh.

Figure 5. Human Portal Vein mesh obtained from the Stl format.

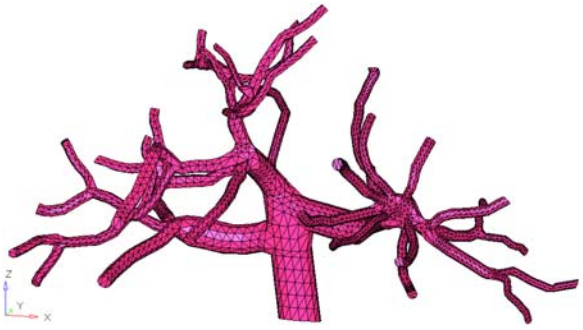

Figure 6. The dragged human vein surface with the help of circles and lines.

In the characterization experiments [18] the Glisson's capsule and vessels were tested under static tension, and elastic moduli were determined for small and large strain along with hyperelastic Ogden material models for each. From the results the Glisson's capsule was modeled with triangular shell elements 0.02mm thick as an elastic material with failure at ultimate strain obtained from the experiment whereas the hepatic veins were modeled as 1mm thick shell elements with Ogden hyperelastic (MAT 77O) material model. The liver parenchyma was characterized in compression [19] and in shear [20] as hyperelastic and viscoelastic material respectively. Therefore, in the model the material properties from the experiments were combined and the liver parenchyma was modeled as solid elements with a hyper viscoelastic material. The inside of the veins was modeled with solid tetrahedral elements in order to reproduce a global-pressurized behavior of vessels with blood. An attempt was made to model these blood elements as liquid material under pressure; however, the model became unstable with such material properties so an elastic material with the elastic modulus of vessels was used. The material models and the parameters used for each are tabulated in Table 1. Again some material properties as stated above were identified after some simulations, such that the model showed realistic behavior. The model was then allowed to fall on a flat base under the influence of gravity so that a flat geometry on a surface was obtained to replicate the real world scenario. The geometry was then extracted and used for further simulations.

The liver model was placed over a rigid plate, of which the nodes were fixed in all 6 degrees of freedom to validate against the Sparks et al. (21) experiments. The impactor and the base plate were modeled as a rigid plate with triangular elements of 280mm wide and 360mm long so as to match the area of the impactor in the experiments which was 1006cm2 and 1mm thick. The impactor was made to weigh 23.4kg as in the experiments by adding additional masses on the nodes. The impactor plate was made to move only in the z-direction and all the other 5 degrees of freedom were constrained. The rigid material properties incorporated for the impactor are also tabulated in Table 1. The surface-to-surface contacts were defined between capsule and top plate, capsule and bottom plate, parenchyma and top plate, parenchyma and bottom plate, and vein and bottom plate. All the contacts were provided with a static friction coefficient of 0.5 and dynamic friction coefficient of 0.4. The impactor plate was supplied with an initial velocity just before impacting the liver as shown in Figure 8 and the contact forces were recorded. It was not possible to compare other values from the experiments so it was decided to compare the peak force for peak strain values mentioned in the experiments.

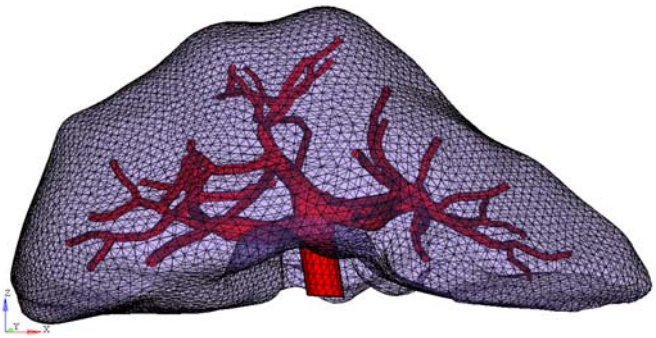

Figure 7. FEM of kidney impacted with a rigid impactor in LS Dyna environment.

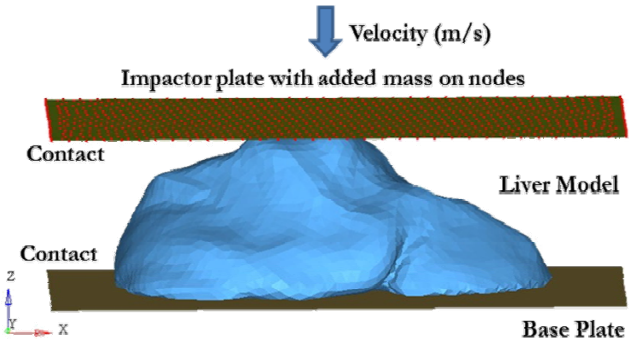

Figure 8.FEM of liver impacted with a rigid impactor in LS Dyna environment.

Table 1. Material model and properties of the modeled liver and kidney

Component	LS Dyna Material Model	Properties
Renal Capsule	*MAT-123 Piecewise linear elastic material*	*RO=0.0011g/mm^3, PR=0.49999, E=50MPa, σ_y=6.9MPa, Failure Strain=0.35*
Cortex	*MAT-077H Soft Tissue Visco Elastic*	*RO=0.001g/mm^3, PR=0.49999, C_{10}=0.02824, C_{01}=0.02886, C_{11}=0.002131, C_{20}=2.31e-4, C_{02}=2.31e-4. G_0=3.77e-4MPa, G_1=6.31e-4 MPa, β_1=0.28e-3 s^{-1}, G_2=7.11e-4 MPa, β_1=3e-3 s^{-1}.*
Glisson's Capsule	*MAT-123 Piecewise linear plasticity*	*RO=0.0011g/mm^3, PR=0.4999, E=160MPa, σy=13MPa, Failure Strain=0.3.*
Hepatic Vein	*MAT-077O Ogden Hyper elastic material*	*RO=0.0011g/mm3, PR=0.4999, μ1=0.0196MPa, α1=10.3043.*
Blood	*MAT-001 Elastic*	*RO=0.0011g/mm^3, PR=0.4999, E=3MPa.*
Parenchyma	*MAT-077H Hyper Visco Elastic*	*RO=0.0011g/mm^3, PR=0.4999, C_{10}=0.0222MPa, C_{01}=0.0214MPa, C_{11}=0.02601MPa, C_{20}=0.021245MPa, C_{02}=0.02672MPa.G_0=3.77e-4MPa, G_1=6.31e-4MPa, β_1=0.28e-3s^{-1}, G_2=7.11e-4MPa, β_2=3e-3s^{-1}.*
Impactor	*MAT 20 Rigid*	*R0=0.008g/mm^3, E=210MPa, PR=0.3.*

III. RESULTS

Kidney

The impact tests were carried out on 9 kidneys at different velocities and the kidneys were analyzed after the impact for the damage. In Table 2 the velocity with which the kidneys were impacted, the peak force sustained by impactor and the damage sustained by each kidney are tabulated. The acceleration of the impactor was also recorded for each kidney and is plotted in Figure 9, whereas the damage propagation recorded by high speed camera and the injury sustained for kidney 6 is shown in Figure 10.

Table 2. Injury outcomes for the kidney impact test.

Kidney	Mass(g)	Impact Velocity(m/s)	Peak Force (N)	Injury
1	38	2.54	1415	Totally smashed, cortex crushed from both sides
2	51	2.01	1074	1 big laceration on capsule and hematoma at the back of the organ along the anvil
3	48	2.02	777	3 small longitudinal laceration on capsule & hematoma along the side and on the lower surface
4	55	2.01	1205	No apparent damage to cortex apart from permanent strain, capsule was lacerated with
5	73	2.4	1979	Totally smashed, side facing anvil was crushed
6	64	1.87	1692	Capsule lacerated from the side facing impactor and 3 big hematoma
7	82	1.54	1402	Capsule suffered less lacerations whereas 1 big and 2 small hematomas where observed on side
8	62	1.54	1348	Side facing anvil was smashed with huge damage to capsule and 3 medium hematomas
9	65	1.54	875	Side facing anvil was smashed with huge damage to capsule and 3 big hematomas

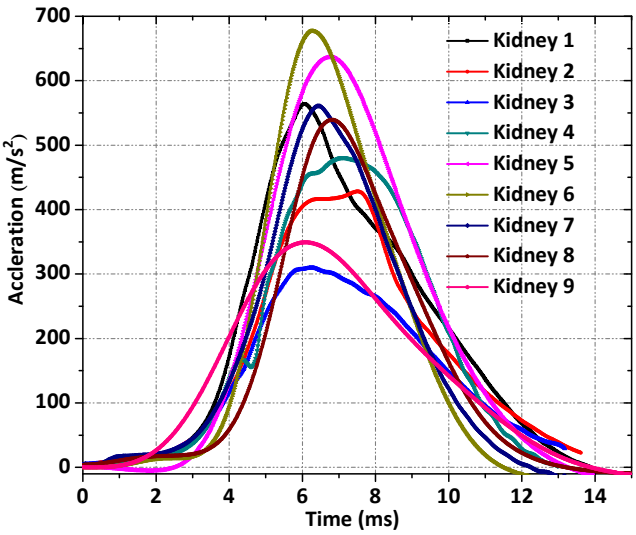

Figure 9. Acceleration plot of the impactor (kidney test).

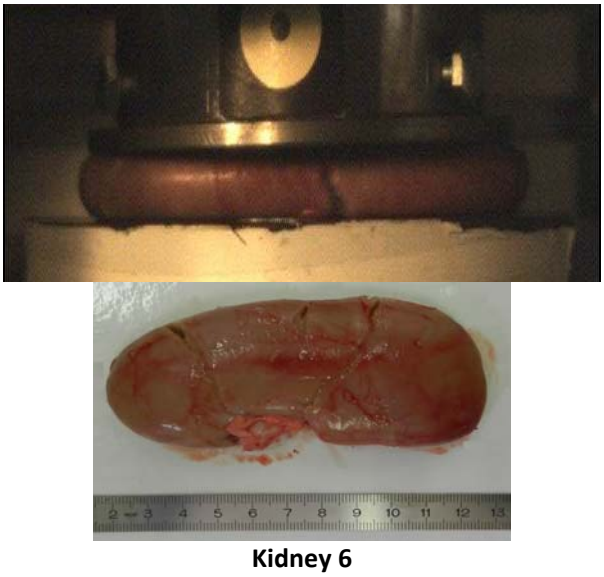

Kidney 6

Figure 10. The experimental representation of fracture of renal capsule during the impact test.

It was observed that, even though the mass of the kidneys and velocity of impact did not change much, there was considerable difference in the acceleration plots (for example kidney 3 & kidney 4, and kidney 8 & kidney 9). This can be due to the difference in the geometries of the kidney and/or the amount of blood inside the kidneys, as some blood was drained out during transportation in some kidneys. However, in the 3rd kidney it can be observed that the acceleration experienced by the impactor is less, which was probably due to the fact that the kidney already had a small cut on one side. In all the kidneys, however, there was maximum damage to the cortex with multiple hemorrhages and lacerations to the capsule.

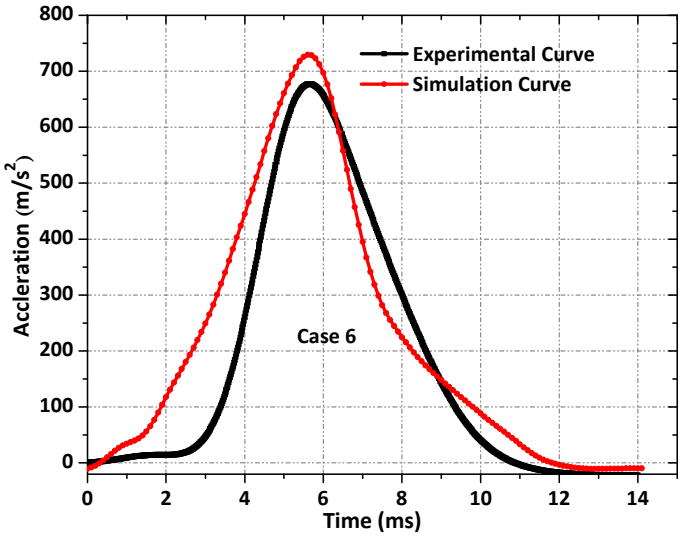

Figure 11. Experimental and simulation acceleration plot for kidney 6

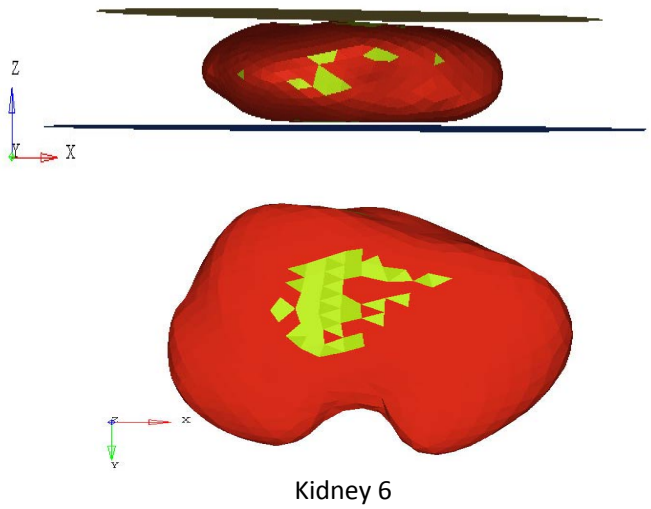

Kidney 6

Figure 12. The analytical representation of fracture of renal capsule during the impact test.

An attempt was then made to simulate the same experiments with the FE model and reproduce the result for each kidney. The calculation time was observed to be 10 minutes on an Intel core 2 duo 3GHz processor with 3 GB ram to simulate 20 milliseconds of impact with LS Dyna solver 'ls971_d_R5.1.1_win32_p'. The comparison of experimental and simulation acceleration of the impactor for kidney 6 is represented in Figure 11 and the comparison for the rest is tabulated in Appendix 1. It shows that even though the initial slope of the simulation acceleration is not exactly in accordance with the experimental curve, the peak value is very comparable, thus generating peak force values similar to that of the experimental results. For the rest of the cases as well, the simulation peak force and acceleration were observed to be in accordance (Appendix 1), except for kidney 3 which is again probably due to the prior damage to the kidney and kidney 5 which can be due to very high impact velocity. The visual description of the fracture of the capsule for experiments and the simulation can be observed to be similar from Figure 10 and Figure 12 for kidney 6. In the simulation it can be observed that the red part, i.e. the renal capsule, is deleted as it was observed in the experiments, thus providing a good visual representation of the injury. The results for all the simulations were observed to be in accordance with the experimental data for the fracture pattern of the capsule. Most of the elements were observed to be deleted from the impact and anvil side as can be seen for Figure 12, along with lacerations on the sides depending on the impact velocity; more the velocity more was the damage.

Liver

In the liver impact experiment, each liver was inspected for injuries on the organ surface and in the organ interior. Injury severity scores were assigned by a trauma surgeon according to the Abbreviated Injury Scale (AIS) from AIS 0 (no injury) to AIS 5 (hepatic avulsion). Peak values of force were defined at the time of maximum liver compression (strain) and are tabulated in Table 3 for all the tests (L6 data are missing). Experimental injury outcomes included shallow lacerations of the liver capsule, deep lacerations, burst-type stellate lacerations and intra-parenchymal damage.

Table 3. Comparison of experimental [21] and simulation peak force for peak strain.

No.	Experimental				Numerical			
	Mass g	Velocity (m/s)	Peak Strain (%)	Peak Force (N)	Without Veins		With Veins and Blood	
					Mass (g)	Peak Force(N)	Mass (g)	Peak Force(N)
HL1	1588	4.3	39	2580	1556	9078	1556	6881
HL2	4660	4.3	32	3966	4616	13174	4669	10489
HL3	1367	4.2	28.2	9223	1334	7802	1378	5189
HL4	1745	5.7	43.1	5799	1708	11062	1761	8509

HL5	1760	2.8	31	7106	1759	7031	1761	5016
HL7	2948	1.8	29	4847	2938	6660	2935	4942
HL8	2139	1.6	31.6	3218	2140	7337	2146	6499
HL9	1722	1.8	34.1	5941	1712	7567	1738	5659
HL10	2293	1.7	32.3	5090	2291	7489	2272	5214
HL11	1646	4.6	26.6	14307	1642	13510	1640	10601
HL12	995	1	20	3262	1009	1860	1000	1374
HL13	1147	5.2	36.6	18302	1164	16470	1132	13726
HL14	1545	2.7	30.5	4283	1554	5438	1558	4586
HL15	2330	2.7	25.6	7406	2321	7246	2317	4869

The same experimental results were obtained from the simulation of the liver under LS Dyna to validate the liver models (with and without veins). For the liver model without vessels the time required to calculate the model took roughly 15 minutes on an Intel core 2 duo 3GHz processor with 3GB ram to simulate 15 milliseconds of impact, whereas time required for each model with vessels and blood was more than 20 hours on the same machine. All the simulations were performed with LS Dyna solver (ls971_d_R5.1.1_win32_p). The peak force required for peak strains for both the models (with and without veins) along with the experimental results are also tabulated in Table 3. In Table 4 the simulation injury in terms of capsule laceration is represented. The Glisson's capsule is represented in red, the liver parenchyma is shown in yellow and the veins are shown in blue. In the simulation, the injuries in terms of laceration can be observed from the deleted capsule elements and can be seen to be comparable to the experimental injuries. The injuries were observed to be close for all the 14 cases (HL6 is missing) to a good extent, and also injuries were not observed for cases with lower velocities in both the experiments as well as in simulations.

Table 4. Comparison of experimental and simulation injuries.

Subject/AIS	**Experimental Injury Description**
Model without Vessels	
HL05/3	Five superficial lacerations on right lobe (3, 5, 5, 6, and 7 cm); Moderate internal damage (5 cm).
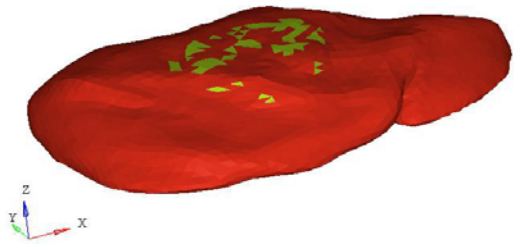 Top View	 Bottom View
Model with Vessels and Blood	
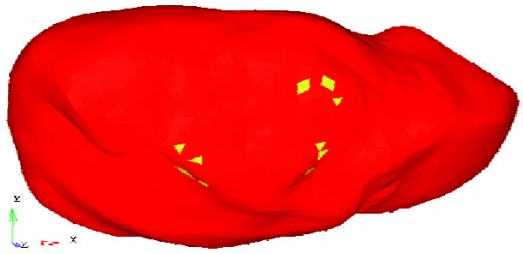 Top View	 Bottom View

IV. DISCUSSION

Kidney

An exclusive set of material parameters for each organ constituent are proposed for the first time in this study. The material parameters for each constituent of the organ in the model were so adjusted to match the experimental fracture pattern for all the cases. The visual description of the fracture of the capsule for experiments and the simulation for kidney 6 can be observed to be similar from Figure 10 and Figure 12. For the rest of the kidneys the renal capsule elements were deleted in similar fashion; for higher impact velocity more elements were deleted suggesting more damage and fewer elements were deleted for lower impact velocities suggesting less damage. The peak force observed by the impactor for experiments is tabulated in Table 2. The percentage error in peak force between the experimental and simulation results is plotted in Figure 13, and it can be observed that the theoretical peak force is in good agreement except for kidney 3. The average error in the peak force for all the results except for kidney 3 and kidney 5 was calculated as 2.9%, whereas the error for all 9 kidneys was around 15.4%. The hour glass energy was observed to be less than 1% which is much less than the prescribed limit of less than 10%. So considering the peak force and injury propagation the model can be considered as a good start and can be used for impact biomechanical applications. However, there is still room for improvement and the material parameters can be modified in a systematic manner by performing a parametric study to achieve more optimal behavior with the model. As the number of material parameters are numerous, it was not possible to perform such an analysis in this study. Also the viscoelastic material parameters used for the kidney model were obtained from shear experiments on liver parenchyma at low frequencies [20], which is not ideal and can be improved by using the material parameters for kidney at higher frequencies.

It can be observed from the material properties (Table 1) that the capsule elastic modulus (50MPa) is on the higher side as compared to the stiffness obtained from the experimental data (16MPa)[19]. The higher stiffness of the elastic modulus was considered after certain iterations, which suggests that the capsule behavior is stiffer when it is attached to the organ. It was also observed that the acceleration plots are greatly affected by geometry in both the experiments as well as the simulations. Considering all these factors, it becomes highly important to have the exact corresponding geometry of the kidney as it can have a great influence on the results. This is also a limitation of this study although the available geometry was scaled for the same dimensions and mass for each case. Also the number of kidneys considered for the impact experiments was not sufficient and more experiments should be performed at different impact velocities to obtain more detailed behavior of the organ under impact. However the boundary conditions such as the coefficient of friction, type of contact etc. did not influence the results, still exact friction coefficient needs to be determined. Also the influence of different mesh sizes can be studied on the results.

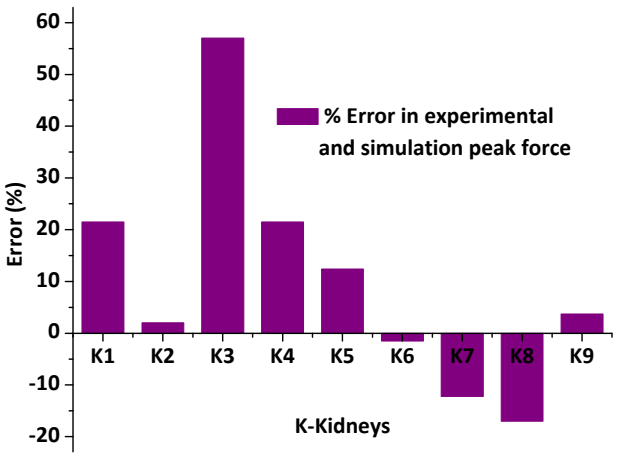

Figure 13. % over estimation of the peak force for kidney FE model.

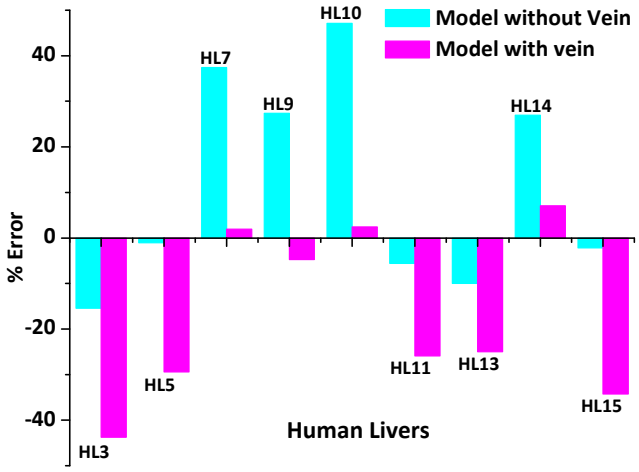

Figure 14. % error for experimental and analytical peak forces for liver model with and without veins.

Liver

This study is a first attempt to develop a human liver model with individual constituents of the organ which can simulate the injuries in a realistic manner. The liver model with the vessels was observed to be less stiff than the model without vessels as can be observed from the comparison of peak force (Table 3). The percentage error **in** the peak forces of experiment and simulation was calculated as the difference between experimental peak force and simulation peak force divided by experimental peak force. In Figure 14 the percentage error between experimental and simulation peak forces are plotted for the two models of liver, except for the cases where the error was observed to be more than 50% (i.e. HL01, HL02, HL04, HL08 & HL12). The cause of having errors on the higher side in these cases can be due to various reasons such as technical defects in experimentation or inexact geometries due to scaling of models. Also, each liver has its own unique properties (geometry, internal venal structure, post mortem time) which could have influenced the results. This can be observed from the experimental results of cases HL01 and HL11. For almost the same velocities and same mass of liver, case HL11 has almost 5.5 times more peak force for less strain. Also, it can be noted that for case HL02 in which the error is maximum, the mass of the liver was very high, and for case HL12 the error for the model without veins exceeded 50%; hence omitted in Figure 14. The remaining 9 cases which produced close results are compared in Figure 14 for the model with and without vessels. It can be observed that for most of the cases for the liver model without vessels, the simulation peak force is overestimated suggesting the liver model to be stiffer, whereas for the model with vessels the simulation peak force is underestimated which suggests that the liver model is less stiff. However, the average error in peak force for 9 cases considered in Figure 14 for liver without vein is 11.6% and is -16.8% for liver model with veins and blood, which shows that the developed model is a good start. In the liver model as well, the hour glass energy was observed to be less than 1% which is well within the prescribed limits.

In the real world there would be failure of parenchyma which will result in lower outcome of forces. But in the LS Dyna it is not possible to reproduce failure for hyper viscoelastic material with the existing laws, thus resulting in more force. However, the degree of damage to the capsule was also compared with the experimental injury description and the visual damage suggested that most of the injuries were sustained by the right lobe as illustrated in the experiments. From Table 4 the degree of injury to the liver for case HL5 can be observed. Ideally the model with vessels should have behaved stiffer as the vein and the blood both were incorporated with stiffer material than parenchyma. But the model behaved less stiff, which can be due to the fact that the blood was considered with elastic modulus of vessels which may not be the case in the real world as blood can have more pressure and hence more stiffness or it may also be due to the geometrical differences. For the model with veins, it can be observed that the injuries in terms of laceration or deletion of the capsule elements are less as compared to the experimental injuries and are also less as that in the model without veins. For the Glisson's capsule the stiffness of the material is considered again on the higher side as for the kidney, thus suggesting that the capsule behaves stiffer when attached to the organ.

In the future more experiments are required to be performed in such a way that the results could be easily reproduced and the material parameters of the models better optimized. Also it is well known that the hexahedral elements best reproduce compression behavior. It would therefore be worth meshing these organs with hexahedral mesh of different mesh sizes though it is a bit complicated because of the complex geometries of the organs.

V. CONCLUSIONS

The first liver and kidney models developed with individual constituents of the organs are proposed. The kidney FE model was used to reconstruct dynamic experiments performed on porcine kidneys and the peak force for the impactor was reproduced using the numerical approach. The kidney models have been shown to be robust for high energy impacts and can be used in biomechanical applications, as injury in the form of lacerations can be reproduced satisfactorily. One limitation of this detailed study, however, is that the geometry of the model was scaled to obtain the desired mass and size instead of using the geometries of the actual kidneys on which the experiments were performed. The results can thus be improved by using the scans of the same organs on which the experiments are performed. Also, larger impact experiments would be helpful to better understand the kidney behavior under impact.

The human liver FE model aims to reconstruct the high energy impacts reported by Sparks et al. [21]. Human liver models with and without veins are proposed for the first time in this study. Like the kidney, these models can reproduce the impact injuries satisfactorily. However, maximum force was observed to vary considerably from experimental forces. Based on this pilot study it is not advisable to use veins unless the phenomenon such as hemorrhage is to be reproduced. However, the proposed model is a good start and can be used for high energy impacts in impact biomechanical applications. The model can also be improved in a similar manner as that of the kidneys by using the geometries of the experimental livers in the liver model.

VI. ACKNOWLEDGEMENT

We would like to acknowledge 'Region *Alsace, France*' and '*Daimler AG, Germany*' for the support of this study. We would also like to acknowledge the support of '*IRCAD France*' for providing the organs as per requirements.

VII. REFERENCES

[1] Augenstein J, Bowen J, Perdeck, E, Singer M, Stratton J, Horton T, Rao A, Digges K, Malliaris A, Steps J, Injury Patterns in Near-Side Collisions, SAE Technical Paper Series 2000-01-0634, 1-9, 2000.

[2] Rouhana SW, Biomechanics in Abdominal Trauma, In Nahum, AM, Melvin JW (eds). Accidental Injury Biomechanics and Prevention, *Springer-Verlag*, New York, 1993.

[3] Lau IV, Horsch JD, Viano DC, Andrzejak DV, Biomechanics of Liver Injury by Steering Wheel Loading, *Journal of Trauma* 27:225-235, 1987.

[4] Carmona RH, Lim RC, Clark GC, Morbidity and Mortality in Hepatic Trauma: A 5 Year Study. *American Journal of Surgery* 144:88-94, 1982.

[5] Elhagediab AM, Rouhana SW, Patterns of Abdominal Injury in Frontal Automotive Crashes. 16th ESV Conference; Windsor, Canada. 1998.

[6] Scollay JM, Beard D, Smith R, McKeown D, Garden OJ, Parks RW, Eleven Years of Liver Trauma: The Scottish Experience. *World Journal of Surgery* 29:744-749, 2005.

[7] Nicolle S, Noguer L, Palierne JF, Shear Mechanical Properties of the Spleen: Experiment and Analytical Modelling. *Journal of the Mechanical Behavior of Biomedical Materials,* 9:130-136, 2012.

[8] Lee J and Yang K, Development of a Finite Element Model of the Human Abdomen. *Stapp Car Crash Journal*, 45:79-100, 2001.

[9] Zhao J, Narwani G, Development of a Human Body Finite Element Model for Restraint System R&D Applications. *Proceedings, 19th International Technical Conference on the Enhanced Safety of Vehicles,* Paper Number 05-0399, 2005.

[10] Zhao J, Narwani G, Biomechanical Analysis of Hard Tissue Responses and Injuries with Finite Element Full Human Body Model. *Proceedings, 20th International Technical Conference on the Enhanced Safety of Vehicles*, Paper Number 07-0354, 2007.

[11] Ruan J, El-Jawahri R, Chai L, Barbat S and Prasad P, Prediction and Analysis of Human Thoracic Impact Responses and Injuries in Cadaver Impacts Using a Full Human Body Finite Element Model. *Stapp Car Crash Journal*, 47:299-321, 2003.

[12] Ruan JS, El-Jawahri R, Barbat S, Prasad P, Biomechanical Analysis of Human Abdominal Impact Responses and Injuries Through Finite Element Simulations of a Full Human Body Model. *Stapp Car Crash Journal* 49:343-66, 2005.

[13] El-Jawahri R, Laituri TR, Ruan JS, Rouhana SW, Barbat SD, Development and Validation of Age-Dependent FE Human Models of a Mid-sized Male Thorax. *Stapp Car Crash Journal,* 54:407–430, 2010.

[14] Huang Y, King AI, Cavanaugh JM, Finite Element Modeling of Gross Motion of Human Cadavers in Side Impact. *Stapp Car Crash Journal*, Vol. 38:35-53, 1994.

[15] Vezin P, Verriest JP, Development of a Set of Numerical Human Models for Safety. *19th International Technical Conference on the Enhanced Safety of Vehicles*, Paper Number 05-0163, 2005.

[16] Iwamoto M, Kisanuki Y, Watanabe I, Furusu K, Miki K, Hasegawa J, Development of a Finite Element Model of the Total Human Model for Safety (THUMS) and Application to Injury Reconstruction. *Proceedings of International Research Council on the Biomechanics of Impact,* Munich, Germany, pp. 31–42, 2002.

[17] Shigeta K, Kitagawa Y, Yasuki T, Development of Next Generation Human FE Model Capable of Organ Injury Prediction. *21st International Technical Conference on the Enhanced Safety of Vehicles, June 15–19, Stuttgart, Germany (2009)* Paper number 09-0111.

[18] Umale S, Chatelin S, Bourdet N, Deck C, Diana M, Dhumane P, Soler LJ, Marescaux J, Willinger R, Experimental in vitro Mechanical Characterization of Porcine Glisson's capsule and Hepatic Veins. *Journal of Biomechanics* 44:1678-1683, 2011.

[19] Umale S, Deck C, Bourdet N, Dhumane P, Soler LJ, Marescaux J, Willinger R, Experimental Mechanical Characterization of Abdominal Organs: Liver, Kidney & Spleen, *Journal of the Mechanical Behavior of Biomedical Materials*, 17:22-33, 2013.

[20] Chatelin S, Oudry J, Périchon N, Sandrin L, Allemann P, Soler LJ, Willinger R. In-vivo Liver Tissue Mechanical Properties by Transient Elastography: Comparison with Dynamic Mechanical Analysis, *Biorheology* 48(2):75-88, 2011.

[21] Sparks, J., Bolte, J., Dupaix, R., Herriott, R., Stammen, J., Donnelly, B., 2007. Using Pressure to Predict Liver Injury Risk from Blunt Impact. *Stapp Car Crash Journal,* 51, 401-432.

[22] Snedeker JG, Niederer P, Schmidlin FR, Farshad M, Demetropoulos CK, Lee JB, Yang KH, Strain-rate Dependent Material Properties of the Porcine and Human Kidney Capsule. *Journal of Biomechanics,* 38:1011–1021, 2005.

VIII. APPENDIX

Appendix 1. Experimental and simulation plots fir kidneys.

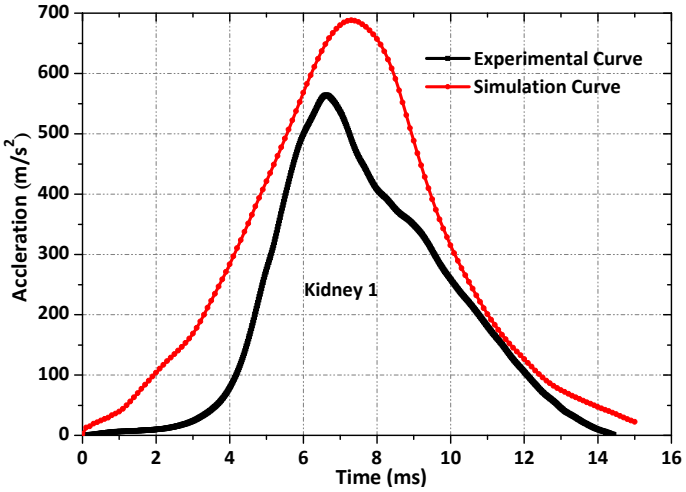

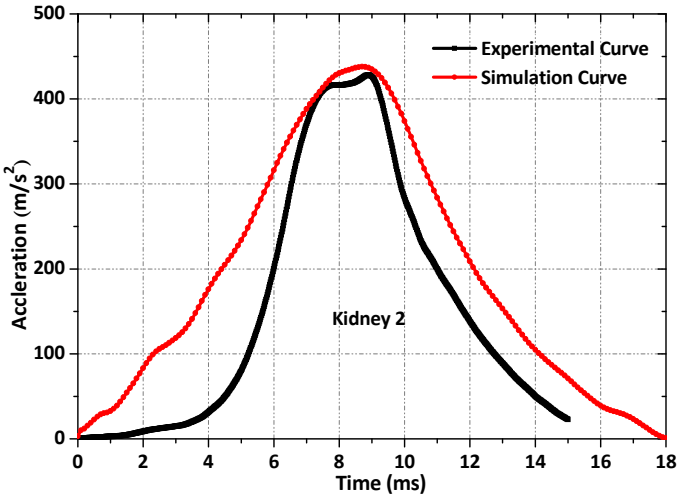

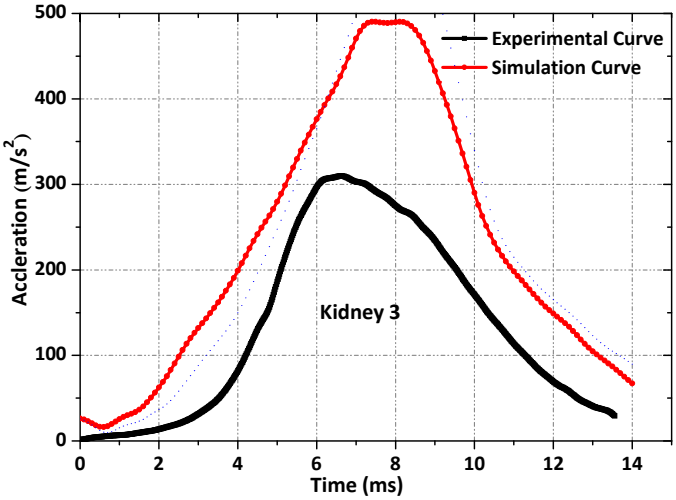

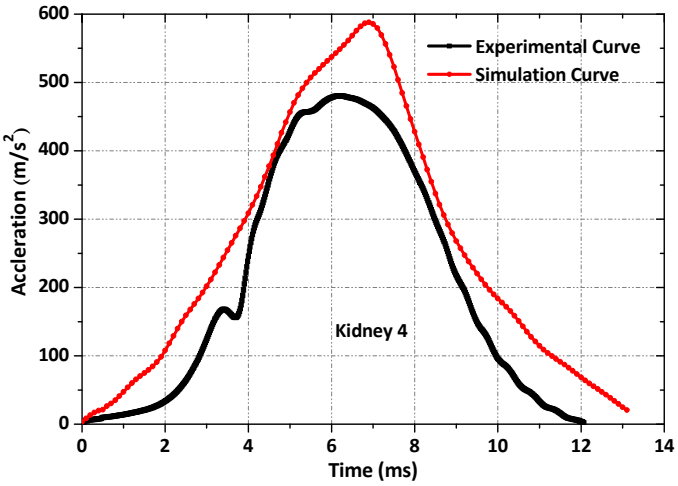

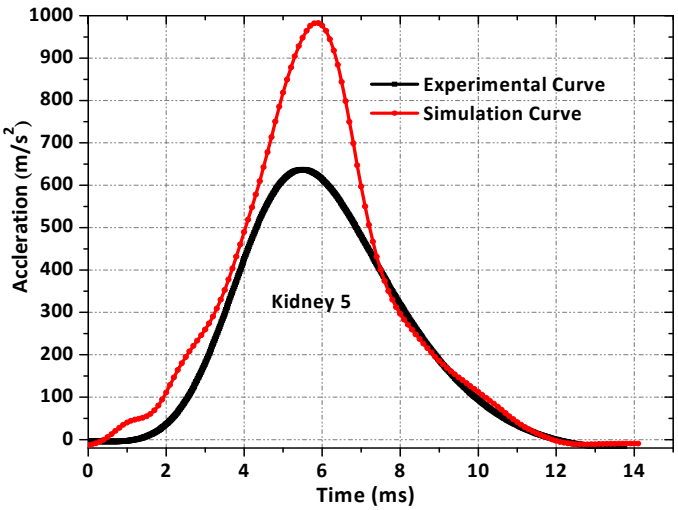

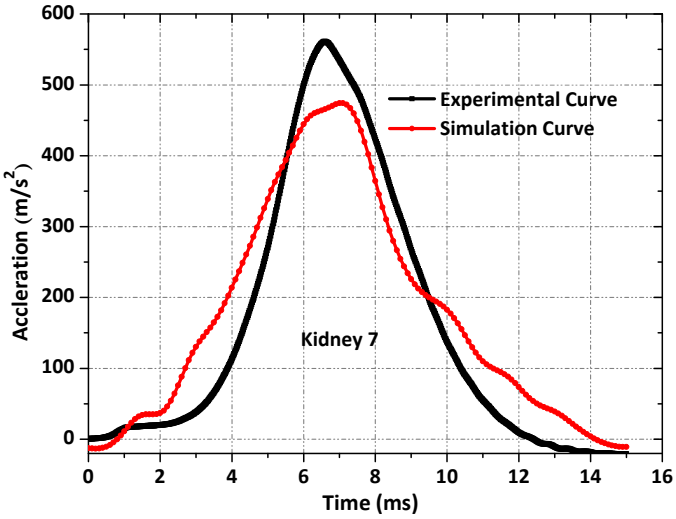

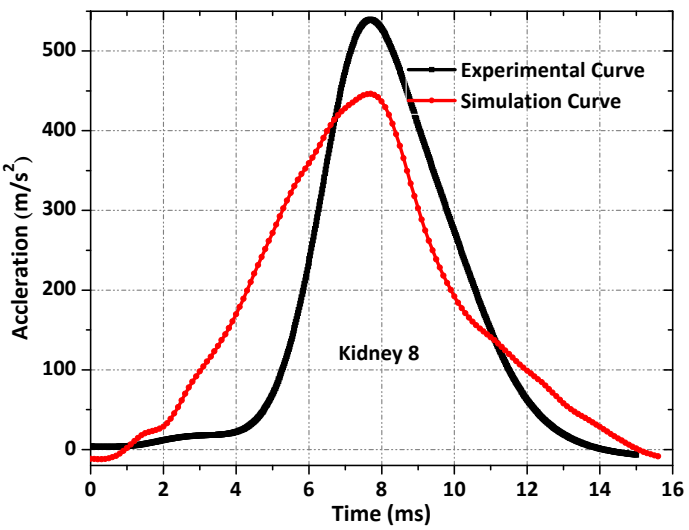

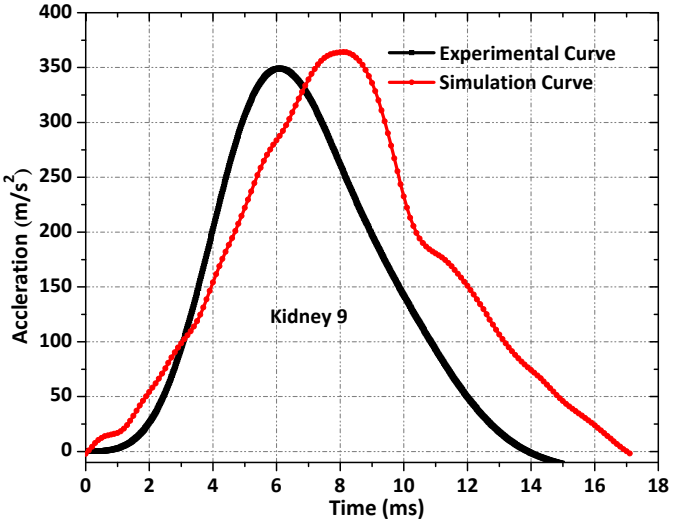

Note: IRCOBI reserves the right to edit and format all conference papers with authors' final approval.